Journal of Reports in Pharmaceutical Sciences 2012, 1(1), 49-59

Formulation Optimization of Low Bioavailable Drug Loaded Alginate Microparticles Using Artificial Neural Networks

Katayoun Derakhshandeh[a,b*], Zahra Hamedi[a], Moin Karimi[a], Mahmood Amiri[c], Farahnaz Ahmadi[d]

[a]Department of Pharmaceutics, Faculty of Pharmacy, Kermanshah University of Medical Sciences, Kermanshah, Iran.
[b]Nano Drug Delivery Research Center, Faculty of Pharmacy, Kermanshah University of Medical Sciences, Kermanshah, Iran.
[c]Medical Biology Research Center, Kermanshah University of Medical Sciences, Kermanshah,Iran.
[d]Department of Pharmacology and Toxicology, Faculty of Pharmacy, Kermanshah University of Medical Sciences, Kermanshah, Iran

ARTICLE INFO

Article Type:
Research Article

Article History:
Received 2012-03-26
Revised: 2012-04-15
Accepted: 2012-04-19
ePublished: 2012-04-25

***Keywords*:**

Alginate
Microparticles
Furosemide
Artificial Neural- Networks
Oral Drug Delivery

A B S T R A C T

In the present study, sodium alginate microparticle for oral delivery of furosemide was designed whether the encapsulation into microparticles might improve the oral absorption of this potent loop diuretic. We described preparation of microspheres based on ionotropic gelation method and characterized its physicochemical properties.To acquire an optimum formulation, a Generalized Regression Neural Networks (GRNN) and a Multi-Layer Perceptron (MLP) were employed. The drug loaded formulation parameters were the input vectors of the GRNN and included the amount of polymer, cross linked agent, volume of external and internal phases. The microparticles drug loading, size and in vitro drug release constitute the output vector of each network. In this way, GRNN and MLP were trained to investigate the functional influence of input variables on the output responses. The results demonstrated that GRNN is promising in providing better solutions for optimization of drug delivery system formulation.The obtained optimum formulation showed a narrow size distribution on an average diameter of 700 ± 50 m and drug loading of more than 75%. The drug release profile illustrates a sustained released pattern and released percent of about 36% in 2 hour. In vitro drug release rate for microspheres was found to be sustained over 24 hours, obeying Higuchi order kinetic. Furthermore, the results of this paper confirmed that alginate microparticles could be a hopeful carrier for orally administration of furosemide and provides a sustained release property for this potent anti hypertension drug. In addition, the novel formulation design facilitates the optimization and successful development of microsphere formulations for enhanced safe and effective oral drug delivery.

[*]**Corresponding author: Katayoun Derakhshandeh**, **E-mail:** Kderakhshandeh@kums.ac.ir

Introduction

Cardiovascular disease (CVD) has recently become the leading cause of death in developing countries. In the last few years, controlled release systems have become increasingly important and present some advantages over traditional pharmaceutical preparations. Indeed, in this case, less active drug is necessary for similar results and consequently less secondary effects and more efficiently used [1].

Furosemide5-(aminosulfonyl)-4-chloro-2- [(furanylmethyl) amino] . benzoic acid is a diuretic and antihypertensive drug, with high ceiling diuretics exerting its action on the cortical thick ascending limb of Henle's loop in the kidney by interfering with the Na^+–K^+–$2Cl^-$ cotransport system at the lumen membrane [2] . This drug is practically insoluble in water [3,4] . and belongs to class IV of BCS system, which has poor and erratic absorption after orally administration, and inter subject variation in pharmacokinetic parameters [5] . Consequently, the encapsulation of these drugs within biocompatible carriers such as micro and nanoparticles, liposomes, micellar systems and conjugates has been proposed as a method to increase their oral bioavailability [6-11] .

Alginic acid is a hetero polysaccharide made of α-L-glucuranic and β-D-manuronic acids and is found in many algae species, especially inside the brown algae. The overall composition and the sequence of monomers in the alginated polysaccharide vary extensively depending on the origin [12,13] . Because of its advantageous biological properties, such as biodegradability, biocompatibility, nontoxicity, high adsorption capacity, good adhesion and sorption, largely contribute to its multiple applications as gelling agent in food industry to encapsulation of living cell [14,15] . This carboxylic polyelectrolyte is soluble in water and precipitates in the form of a coacervate in the presence of multivalent metal ions like Ca^{2+}, Co^{2+}, Zn^{2+},Ba^{2+}, Fe^{2+}, Fe^{3+}, and Al^{3+}.[16,17] . (Fig.1)

Several important factors contribute to the effectiveness of this method in preparing particles with acceptable size range, shape and the percentage of the drug load, namely the concentration of polymer and crosslinker and volume of internal and external phases. It is difficult to assess the effect of the variables individually or in combination, therefore deriving a mathematical model suitable for establishing a quantitative relationship between the formulation variables is necessary [18-20] .

Recently, there has been increased interest in applications of artificial neural networks (ANNs) in biomedical researches [21,22] . ANNs are used in pharmaceutical and pharmacokinetic areas to model complex relationships and to predict the nonlinear relationship between causal factors and response variables. The distinct features of the ANN make this approach very useful in situations where the functional dependence between the inputs and outputs is not clear.

The Multy-Layer Perceptron (MLP) has played a central role in the research of neural networks.

The study began with the nonlinear and adaptive response characteristics of neurons and it was discovered that the MLP is a universal approximate agent of relations between inputs and outputs variables [23] . This model is a generalization of both radial basis function networks (RBFN) and probabilistic neural networks that can perform linear and nonlinear regression [24] . These feed-forward networks use basis function architectures that can approximate any arbitrary function between input and output vectors directly from training samples, and they can be used for multi-dimensional interpolation [25] .

Although Generalized Regression Neural Network (GRNN) are not as commonly used as RBFNs or MLP networks, they have been applied to solve a variety of problems including prediction, control, plant process modeling or general mapping problems

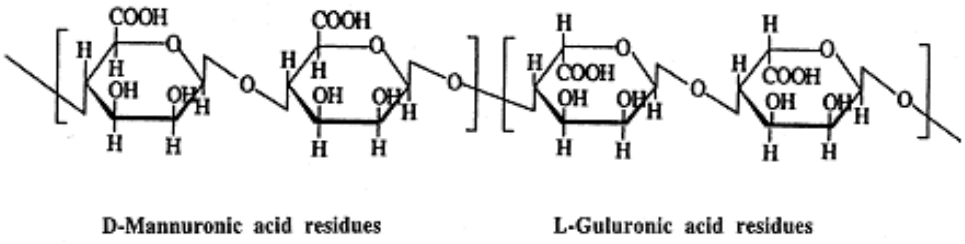

Fig. 1. The molecular structure of furosemide and Structure of alginate showing both β-D-mannuronic acid and α-L-guluronic acid residues.

[26] . GRNN has the advantage of being easily trained and required only one free parameter.

In the present research, alginate microspheres of furosemide using ionotropic gelation method are designed and developed, whether the encapsulation into microparticles might improve the oral absorption of this potent loop diuretic. To obtain an optimum formulation, the GRNN and

MLP neural networks were employed to obtain optimum formulation and experimental data sample collected from in vitro characterization.

Materilas and Methods

Chemicals and reagents

Furosemide was received as a gift sample from Atra Co. (Tehran, Iran). Sodium alginate and calcium chloride were purchased from Sigma (Oakville, Canada). All other chemicals and solvents were of analytical grade satisfying pharmacopoeial specifications.

Preparation of alginate gel microspheres

Alginate microspheres were prepared by ionotropic gelation technique. Sodium alginate in different concentration was dissolved in distilled water under vigorous agitation. The drug was added to aqueous solutions of sodium alginate and stirred up to complete dissolution. This solution was dropped using a hypodermic syringe into a second solution, containing $CaCl_2$ with different ratios and cure for 15 min. After the microspheres formed, were filtered and washed with distilled water, and dried in oven at 37^{o}C for 48 h (Fig. 2).

The drug loaded formulation parameters are the independent variables and include sodium alginate concentration (*X1)*, $CaCl_2$ concentration (*X2)* and volume of internal and external phases (*X3, X4*) (Table 1).

On the other hand, the drug loading (*Y1)*, size of microspheres (*Y2*) and the amount of released drug in 2 h (*Y3*) are the response and dependent variables (Table 2).

To achieve an optimum formulation, MLP and GRNN are employed to investigate the functional dependence of input variables on the output response [27,28] .

Percentage of formulation yield and drug entrapment efficiency

The yield was calculated as the weight of the microspheres recovered from each batch di vided by total weight of drug and polymer used to prepare that batch multiplied by 100.

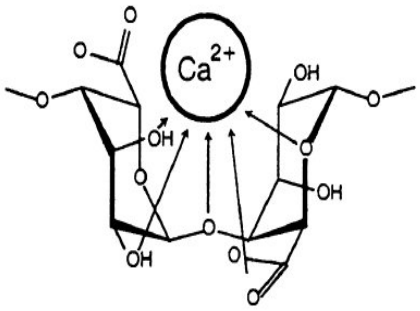

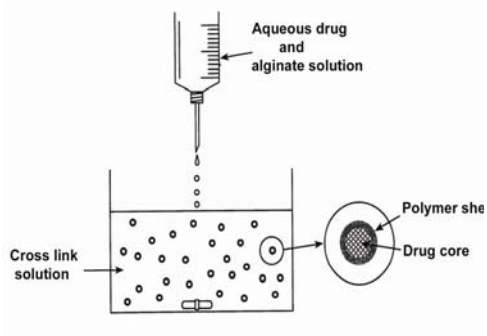

Fig. 2. Schematic representation of alginate microspheres were prepared by ionic gelation method.

Table 1. Factorial design parameters and experimental conditions.

Factors	Low level	High level
X_1: concentration of sodium alginate (%)	0.8	4
X_2: concentration of $CaCl_2$ (%)	1	6
X_3: volume t of internal phase (ml)	15	30
X_4: volume of external phase (ml)	20	75

The drug entrapment efficiency was calculated as 10 mg of furosemide microspheres were added to 10 ml of isotonic phosphate buffer (pH 7.4) under sonication for 20 min. Then microspheres were magnetically stirred to promote swelling and breakup of the cross-linked structure. The solution was filtered and the aqueous solution was assayed by UV spectrophotometer at the max wave length value of 273 nm using a regression equation derived from the standard calibration curve graph (r^2=*0.9954*). The drug entrapment efficiency (DEE) was calculated by the following equation:

$DEE\ (\%) = P_c/T_c \times 100$ (1)

Where *Pc* is practical content and *Tc* is the theoretical content. All the experimental units were analyzed in triplicate (*n=3*).

Particle size determination

Particle size of the prepared microsphere was determined using an optical microscope (ModelBM-22h) fitted with a stage and an ocular micrometer. Hundred dried microspheres were measured for calculating the mean diameter of microspheres.

Table 2. Experimental design and percentage of drug loading, size and microparticle yield responses (n = 3)

Run	X_1 (%)	X_2 (%)	X_3 (ml)	X_4 (ml)	Y_1 (%)	Y_2 (um)	Y_3 (%)
F1	1.20	1.00	15.00	20.00	10.00±0.50	500.15±51.20	41.26±4.66
F2	1.50	2.00	25.00	50.00	52.00±0.64	550.11±50.10	53.24±2.56
F3	2.00	1.50	25.00	50.00	61.22±0.75	600.14±49.25	68.29±1.25
F4	2.00	2.00	25.00	50.00	63.10±0.91	621.14±50.05	68.15±3.85
F5	2.00	2.50	25.00	50.00	64.12±0.95	650.45±50.17	69.23±6.59
F6	2.50	1.00	25.00	50.00	56.12±0.85	670.27±52.41	60.48±7.65
F7	2.50	1.50	25.00	50.00	60.81±0.94	700.09±33.15	42.14±3.34
F8	2.50	2.00	25.00	50.00	65.45±0.87	705.34±28.46	63.26±3.78
F9	2.50	2.50	25.00	50.00	74.25±0.92	750.24±42.15	62.49±5.61
F10	2.50	3.00	25.00	50.00	79.58±0.75	800.07±35.67	55.58±5.59
F11	2.50	2.50	15.00	50.00	60.23±0.91	850.27±34.25	59.45±4.25
F12	2.50	2.50	25.00	75.00	62.21±0.94	854.11±43.65	49.26±7.21
F13	2.50	6.00	25.00	25.00	58.10±0.89	873.27±41.27	54.33±6.98
F14	3.00	1.50	25.00	50.00	49.21±0.92	850.78±40.25	46.85±6.31
F15	3.00	2.00	25.00	50.00	54.21±0.94	907.58±39.57	52.18±5.36
F16	3.00	2.50	25.00	50.00	60.52±0.84	935.67±43.57	45.54±2.52
F17	3.00	3.00	25.00	50.00	64.61±0.95	1010.25±74.21	40.27±3.56
F18	3.50	2.00	25.00	50.00	50.09±0.87	1205.08±69.74	35.64±2.25
F19	4.00	3.00	30.00	50.00	44.90±0.94	1350.08±97.25	28.67±4.50
F20	4.00	3.00	20.00	50.00	70.27±0.90	1200.89±49.67	36.33±7.21

In-vitro drug release study

In vitro drug release study was carried out in type I dissolution test apparatus using phosphate buffer (pH 7.4), simulated gastric fluid (SGF pH 1.2) and simulated intestinal fluid (SIF pH 7.4) as dissolution medium. Volume of dissolution medium was 500 ml and temperature was maintained at (37°C) throughout study. Basket speed was adjusted at 50 rpm. In predicted time interval, 5 ml of sample was withdrawn with replacement of fresh medium and analyzed for furosemide content by UV-Visible spectrophotometer at 273 nm. According to factorial design offers, twenty formulations were done and the responses were evaluated (Table 2). Indeed, the data of this table constitute the training and validation data sets which are used to obtain the optimum formulation. The variables X_1-X_4 are the four input variables of the ANN while the variables Y_1-Y_3 represent the output variables of the network (four inputs and three outputs).

Differential scanning calorimetry (DSC)

The physical state of the microparticles components was characterized by thermal analysis in DSC-60 analyzer (Shimadzu Co., Kyoto, Japan). Samples (10 mg) were sealed into aluminum pans and heated in an inert atmosphere of nitrogen with a heat rate of 10°C/min. Calibration of the system was performed using octadecane and indium.

In vitro drug release kinetics

In order to determine the release model which best describes the pattern of drug release. Data were analyzed with the following release models: zero order

(Eq. 2), first order (Eq. 3), Higuchi (Eq. 4), and Peppas and Korsemayer (Eq. 5).

$$Q.\ t = k_0.\ T \quad (2)$$
$$LnQ_t = lnQ_0 - k_1.t \quad (3)$$
$$Q_t = k_H.\ t_{1/2} \quad (4)$$
$$M_t/M_\infty = K.\ t_n \quad (5)$$

where Q_t is the amount of drug released in time t, Q_0 is the initial amount of drug in the microspheres, M_t corresponds to the amount of drug released in time t, M_∞ is the total amount of drug that must be released at infinite time, K is a constant and n is the release exponent indicating the type of drug release mechanism. If n approaches 1, the release mechanism is zero order. On the other hand, if $0.5 < n < 1$, non-Fickian transport is the case.

The preference of a certain mechanism was based on the correlation coefficient (r^2) for the studied Parameters, where the highest correlation coefficient is preferred for the selection of mechanism of release [28,29].

Neural Network Models

ANNs are characterized in principle by a network topology, a connection pattern, neural activation properties and train strategy. The rapid development of ANN technology in recent years has led to an entirely new approach for biomedical applications. In this section, two types of neural networks that are MLP and GRNN are briefly explained. These networks will be used in the next section to obtain the optimum formulation.

Multi-Layer Perceptron (MLP)

An MLP, illustrated in Fig.3, is used as a first structure for simulations. In the conventional structure of an MLP, a neuron receives its input either from other neurons or from external inputs (input vector). A weighted sum of these inputs constitutes the argument of a nonlinear activation function. The resulting value of the activation function is the neural output. In Fig.3, the output Y of the MLP is a vector with n components determined in the terms of m components of an input vector X and l components of the hidden layer. The mathematical representation may be expressed as:

$$y_i = \sum_{j=1}^{l} \left[v_{ij}\ \sigma\left(\sum_{k=1}^{m} w_{jk}\ x_k + b_{wj} \right) + b_{vi} \right] \qquad i = 1,\ldots,\ n \quad (6)$$

Where v_{ij} and w_{jk} are synaptic weights, x_k is k_{th} element of the input vector, $\sigma(.)$ is an activation function and b is the bias which has the effect of increasing or decreasing the net input of the activation function depending on whether it is positive or negative, respectively. It has been shown that the MLP with tanh nonlinearity or other monotonic nonlinearities is a universal approximate agent or to any arbitrary input-output mappings provided that some reasonable conditions on the nonlinear mapping are satisfied [27].

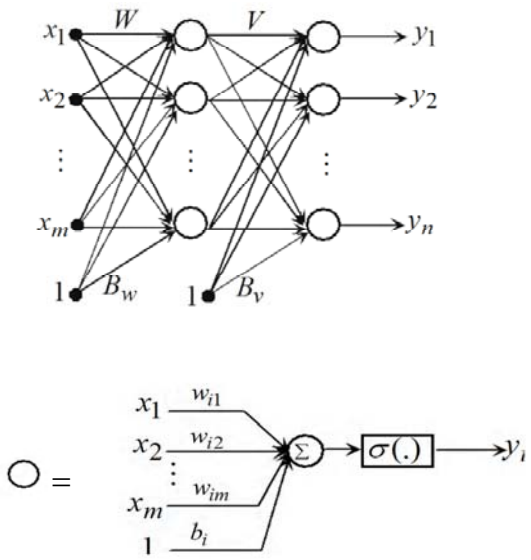

Fig. 3. The MLP Structure

Generalized Regression Neural Network (GRNN)

GRNNs belong to the class of neural networks widely used for the continuous function mapping.

The main function of a GRNN is to estimate a linear or nonlinear regression surface on independent variables (input vectors) U, given the dependent variables (desired output vectors) X. That is, the network computes the most probable value of an output, x^, given only training vectors U. Specifically, the network computes the joint probability density function of U and X. Then the expected value of X given U is expressed as: [24].

$$E[X|U] = \frac{\int_{-\infty}^{\infty} X\, f(U,X)\, dX}{\int_{-\infty}^{\infty} f(U,X)\, dX} \quad (7)$$

An important advantage of the GRNN is its simplicity and fast approximation procedure [28]. In addition, the training process with a GRNN-type algorithm is

much more efficient than with the BP-NN algorithm. The topology of a GRNN is described in Fig. 4.

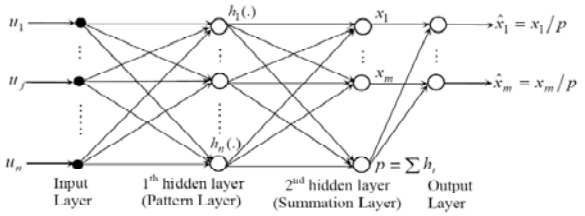

Fig. 4. The GRNN architecture.

Table 3. Mean prediction errors of the individual output variables for each neural network.

Network	MPE of the Y_1	MPE of the Y_2	MPE of the Y_3	Average MPE
MLP	0.1483	0.2103	0.1923	0.1836
GRNN	0.1109	0.1879	0.1384	0.1457

Optimization of drug delivery system formulation

To find the optimum formulation, at first, GRNN and MLP are trained using the data sample listed in Table 2. In so doing, we divided the data samples into two groups, the training and validation data sets. The training group contains 17 randomly selected samples from Table 2 and the validation group includes the other three remaining samples. There are significant variations in the scales of the values of the second input variables. These different scales of the inputs led to ill-conditioning of the problem and hence the ANN could not be trained efficiently. To avoid this problem, all the data listed in Table 2 are normalized to the range of [-1, 1] . before training of the networks. The selection of suitable network architecture is another important factor, since it affects the network convergence as well as the accuracy of estimations [32] .

There exist no analytical methods to determine the optimum number of neurons required for a specific problem [21] . Several rules of thumb to select the number of hidden neurons in an ANN have been proposed by various researchers [22] . It should be mentioned that the number of hidden neurons generally depends on many factors, especially the distribution of training data and the number of data samples. However, in this work, MLP network was trained with a different number (from three to seven) of hidden neurons. The error value is high when the number of neurons is low; in addition, increasing the number of hidden neurons decreases the final error value and makes the network move towards the global minimum. However, when we have more than four neurons in the hidden layer, over-fitting occurs. In this case the number of network parameters that should be adjusted through the learning algorithm is more than the required ones. Therefore, four neurons are required in the hidden layer which leads to the fast convergence and stable minimum error.

To train GRNN, after several simulations and based on trial and error method, $\sigma=0.5$ was selected. To evaluate the performance of each trained network, according to Rafienia and colleagues, [10] . we calculated the mean prediction error (MPE) as defined by:

$$MPE = \frac{\sum(x_i - \hat{x}_i)}{n} \qquad (8)$$

Where xi and x^ are the target value and the estimated value of the variable by the ANN, respectively and *n* is the number of validation data sample. This quantity was computed for each of the validation sample. In this case, we had three MPEs, in which their mean value was used as an index to evaluate the trained neural network performance. For this criterion, the mean value error of the individual outputs for each network is shown in Table 3. The average mean prediction error (AMPE) for each network is also shown in Table 3. Since, different executions of the MLP network leads to the different MPEs, this process should be repeated several times to guarantee the accuracy of the neural network response. Hence, 10 trials were executed for the MLP network. The variance of the aforementioned process for the first, second and the third output variables respectively, which are about 0.1, 0.2, and 0.12%. This confirms the accuracy of the estimations for the MLP network. Noteworthy that there is no need to carry out this process for the GRNN, since the performance of this networks will not changed during different trials. In fact, this is one the main advantages of the GRNN. It does not depend on the different execution.

As can be seen in Table 3, the performance of the GRNN network in estimation of output variables is better than the MLP performance. When the MLP and GRNN were trained, we used the lower and upper limits of the input variables given in Table 1 to partition the input space into smaller regions. In this way, the interval between upper and lower limits of each input variable is divided into several segments. In this research, for the first input variable X_1, the interval [0.8, 4] . is divided into 32 segments with each step length equal to 0.1. For the second, third and fourth input variables the step lengths are 0.1, 2.5 and 5, respectively. Next, the values of these

segments constitute the input vector of trained MLP or trained GRNN to produce the corresponding outputs. Since we want to optimize the output variables such that the drug loading
(Y_1) to be maximized and at the same time the size of microspheres (Y_2) and the amount of release drug in 2 h (Y_3) to be minimized, we define the following cost function:

$$J = Y_2 + Y_3 - Y_1 \quad (9)$$

Based on this definition, minimizing the cost function J corresponds to the minimization of Y_2 and Y_3 and maximization of Y_1.
In this way, we will find the optimum value of the input variables (X_1-X_4) such that the output variables (Y_1-Y_3) which produced by the trained MLP or GRNN minimize the cost function (Eq. 11). Since the performance of the trained GRNN to minimize (Eq. 9) is superior to the performance of the trained MLP, the results of this network are only mentioned in Table 3. Therefore, in this application, GRNN can effectively approximate the function between input and output vectors to find the optimum formulation and is more reliable than MLP.

Results

The furosemide loaded microspheres were prepared by ionotropic gelation method. The microspheres obtained under these conditions were mostly spherical without any aggregation.
Chemical reaction between sodium alginate and calcium chloride to form calcium alginate was utilized for microspheres (Fig 4).To acquire an optimum formulation with minimum experimental and time consuming, statistical artificial neural network was implied.

Microparticle physicochemical characterization

The optimum formulation of alginate microsphere obtained by the GRNN was:
Alginate (3.1%), $CaCl_2$ (2.5%), internal and external phases of 20 and 50 ml, respectively.
This formulation showed a narrow size distribution with an average diameter of 700 ± 50μm, and drug loading of more than 75%. The drug release profile showed a sustained released pattern about 36% in 2 hour. In vitro drug release rate for microspheres was found to be sustained over 24 hours, obeying Higushi order kinetic.

Morphological and size characterizations

Morphology of the various formulations of alginate microspheres prepared was found to be discrete and spherical in shape (Fig.5).
The mean particle size of the various formulations was between 500 and 1200 μm (Table 4). The best formulation showed a narrow size distribution an average diameter of 700 ± 50 μm. The results indicated the proportional increase in the mean particle size of the microspheres with increasing amount of sodium alginate in the formulations.
This could be attributed to an increase in the relative viscosity at higher concentration of sodium alginate and formation of large droplets during addition of the polymer solution to the cross linking agents. Air-dried microspheres were of a larger size than those oven-dried due to incomplete dehydration as a result of air-drying process.

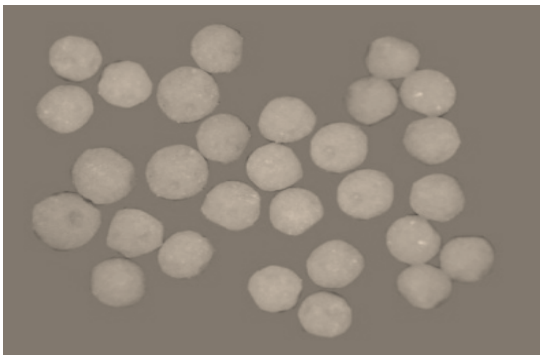

Fig. 5. Macroscopic aspect of furosemide-containing alginate microspheres.

Table 4. Computed kinetic release parameters for the optimum formulation.

Formulation Code	r^2 (Regression coefficient)				N
	Zero Order	First Order	Higushi	Korsmeyer- Peppas	Korsmeyer-Peppas
F*	0.7	0.9241	0.9816	0.9367	0.23

Drug entrapment efficiency of microspheres

The incorporation efficiency increased progressively with increasing sodium alginate concentration (Table 2). An increase in the alginate concentration resulted in the formation of larger microspheres entrapping greater amounts of the drug.
This may be attributed to the greater availability of active calcium-binding sites in the polymeric chains and, consequently, the greater degree of

cross-linking as the quantity of sodium alginate increased (1.5-3% w/v). The low incorporation efficiency of alginate beads cross-linked with Ca^{2+} could be attributed to the formation of porous beads ensuring the diffusion of the drug out of the beads at the time of curing (<1.5%). In amount of (>3% w/v) because high viscosity of polymer, drug cannot correctly loaded in polymer.
The formulation yield in all experiments was upper than 93±5%.

Differential scanning calorimetry (DSC)

The graphs of DSC were shown in Fig. 6. As demonstrated in the graphs, furosemide exhibited a characteristic, sharp exothermic peak at 220 ºC which is associated with an initial and small melting point followed by a sharp decomposition peak of the drug. The alginate polymer (graph b) show a endothermic wide pick at 102 ºC that indicates glass Transition Temperature (T_g) point of polymer and decomposition peak at 230-250 ºC. From the graph (c), we can find easily that the physical mixture of drug with carrier material had two peaks at 220 ºC and 102ºC respectively.

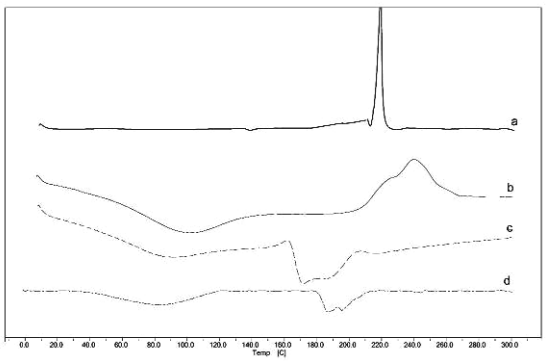

Fig. 6. The DSC graphs of: A) pure furosemide, B) pure Alginate, C) microspheres contained drug, D) microsphere without drug

These results indicated that their properties were kept in physical mixture. According to the graph (c and d), represent that the properties of drug disappeared. The reason should be explained that the microparticles were formed and the drug crystal structure changed to amorphous state. The endothermic peaks at 170-200 ^{o}C, shows a significant effect of crosslink agent on alginate structure.

In vitro dissolution and release kinetic models

All the formulations found to release furosemide in a controlled manner over six hours. To study the effect of sodium alginate concentration on furosemide release, it was used at four different concentrations (1.5-3.5 % w/v). The release profiles are shown in Fig 7.

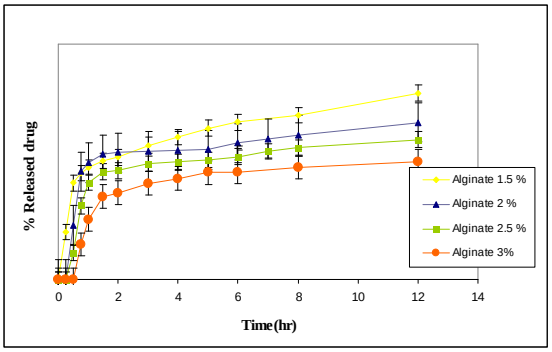

Fig. 7. Effect of sodium alginate concentration on release characteristics of furosemide in phosphate buffer pH 7.4. (mean ± SD, n = 3).

The results indicated the more sustained effect with an increase in the concentration of sodium alginate. It is observed that the steady state release was achieved after an initial lag time and it was directly proportional to the concentration of polymers, principle of gelation by calcium chloride is based on the formation of tight junction between the guluronic acid residues. This increasing in the apparent cross linking density delayed the alginate gel disintegration in phosphate buffer due to the retardation of Ca^{2+} exchange with Na^{+} and eventually increasing lag time. Increased alginate gel density per unit volume was also thought to affect the decreased pore size within the gels, and thus furosemide release becomes slow.
The rate of release has been prolonged with increasing $CaCl_2$ concentration. That can be explained by considering the structure of the gel microspheres. Low Ca^{2+} concentration leads probably to a loose gel, so, the drug can be easily released from the carrier (Fig 8).
The in vitro dissolution data were analyzed by different kinetic models in order to find out the *n* value, which describes the drug release mechanism. The results revealed that furosemide release from in the

phosphate buffer followed Higuchi diffusion (Table 4).

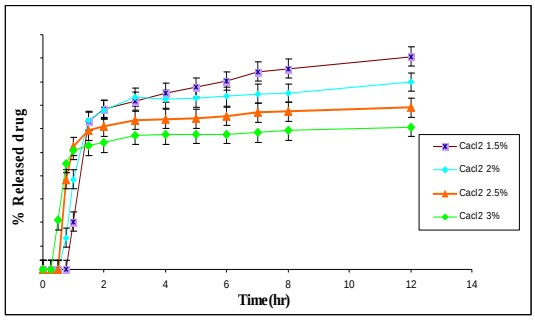

Fig. 8. Effect of CaCl2 concentration on release characteristics of furosemide in phosphate buffer pH 7.4. Bars indicate ±SD (n = 3).

The values of *n* for the release of furosemide from the best formulation, indicating that the drug release from the microspheresfollowed the anomalous fickian diffusion mechanism controlled by swelling and relaxation of the polymer chains.

Fig. 9 shows the release behavior of furosemide from alginate microspheres in SGF (pH 1.2) and SIF (pH 7.4). Approximately, 12% of the drug was released in the SGF over a period of 3 h and 70% in SIF in 24 h. It is generally seen that when microspheres of hydrophilic polymers are immersed in water, they swell and form a gel diffusion layer that hinders the outward transport of the drug, hence, producing a controlled release effect. However, at acidic pH the alginate microspheres shrink due to tightening of the gel meshwork.

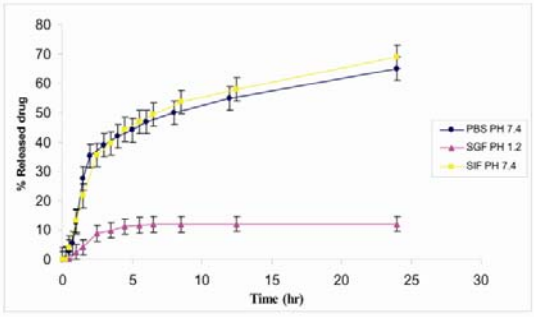

Fig. 9. Drug release profile of optimized formulation in SGF pH 1.2 and SIF pH 7.4. Bars indicate SD (n = 3).

The best-fit model for drug release from microspheres was the Higuchi's matrix model (Table 4). The polymer is eroded at alkaline pH and the contents are released in a sustained manner by both diffusion and slow erosion of polymer matrix.

Discussion

In this paper, it was verified that furosemide loaded alginate microspheres can be utilized for oral administration using the ionotropic gelation method. The chemistry and relatively mild cross linking conditions of alginate have enabled this naturally occurring biopolymer to be used for the encapsulation of a wide variety of drugs. Various therapeutic agents such as antidiabetic, [33] · anti-inflammatory, [34] · antibiotics, [35] · proteins and enzymes [36] · have been incorporated in polysaccharides microsphere to achieve a controlled release system. To acquire the optimum formulation for drug delivery system, an ANN-based approach is proposed. Considering the drug loaded formulation parameters including the amount of polymer, cross linked agent, volume of external and internal phases as the input variables and drug loading, size and in vitro drug release as the output variables. MLP and GRNN were trained to estimate the nonlinear correlation between the input and output spaces. Indeed, the potential of these two networks to obtain the optimum values for input variables were compared. It would appear that performance of the trained GRNN to minimize the cost function is superior to the performance of the trained MLP and is more reliable than MLP to final optimum formulation for drug delivery system.

Controlled release microspheres were successfully prepared and characterized. Microspheres are spherical in shape and having a smooth surface. The drug entrapment capacity is about 75%. The microspheres were found to be effective in sustaining the drug release more than 12 hours. Drug release was diffusion controlled and followed Higuchi order kinetic. The process of drug release from the polymer-drug matrix involves gelation of the polymer, dissolution of the drug, and diffusion of drug through resultant hydrated layer.

The results of this paper showed that utilizing ANN to obtain optimum formulation needs fewer experiments which may present new opportunities for the development of easy, reproducible and cost effective method in drug delivery applications. In sum, the application of the ANNs in biomedical research will definitely increase in the near future. However, the point which is noteworthy is the fact that there is no single modeling approach to address all requirements.

Conflict of interest

Authors certify that no actual or potential conflict of interest in relation to this article exists.

Acknowledgment

We gratefully acknowledge Vice Chancellor for Research and Technology, Kermanshah University of Medical for their financial support. This work was performed in partial fulfillment of the requirements for a Pharm. D of Zahra Hamedi in the Faculty of Pharmacy, Kermanshah University of Medical Sciences Kermanshah-Iran.

References

[1] Aceves JM, Cruz R, Hernandez E. Preparation and characterization of Furosemide-Eudragit con-trolled release systems. Int. J. Pharm. 2000;1:45–53.
[2] Luddens H, Lang HJ, Korpi ER. Structure-activity relationship of furosemide-derived compounds as antagonists of cerebellum-specific GABA;A: receptors. Eur. J. Pharmacol. 1998;344:269–277.
[3] Devarakonda B, Otto DP, Judefeind A, Hill RA, Villiers MM. Effect of pH on the solubility and release of furosemide from polyamidoamine ;PAMAM: dendrimer complexes. Int. J. Pharm. 2007;10:142–153.
[4] Ai H, Jones SA, Villiers MM de , Lvov YM. Nanoencapsulation of furosemide microcrystals for controlled drug release. J. Control. Release. 2003;86:59–68.
[5] Lindenberg M, Kopp S, Dressman JB. Classi-fication of orally administered drugs on the World Health Organization Model list of Essential Medicines according to the biopharmaceutics classification system. Eur. J. Pharm. Biopharm. 2004;58:265–278.
[6] Brigger I, Dubernet C, Couvreur P. Nanopar-ticles in cancer therapy and diagnosis. Adv. Drug. De-liv. Rev. 2002;54:631–651.
[7] Dadashzadeh S, Derakhshandeh K, Shira-zi FH. 9-nitrocamptothecin polymeric nanoparticles: cyto-toxicity and pharmacokinetic studies of lactone and total forms of drug in rats. Anticancer. Drugs. 2008;19:805–811.
[8] Derakhshandeh K, Soheili M, Dadashzadeh S, Saghiri R. Preparation and in vitro characterization of 9-nitrocamptothecin-loaded long circulating nanopar-ticles for delivery in cancer patients. Int. J. Nanomedi-cine. 2010;5:463–471.
[9] Drummond DC, Meyer O, Hong K, Kir-potin DB, Papahadjopoulos D. Optimizing liposomes for delivery of chemotherapeutic agents to solid tumors. Pharmacol. Rev. 1999;51:691–743.
[10] Onishi H, Machida Y, Machida Y. Antitumor properties of irinotecan-containing nanoparticles pre-pared using poly;DL-lactic acid: and poly;ethylene glycol:-block-poly;propylene glycol:-block-poly;ethylene glycol. Biol. Pharm. Bull. 2003;26:116–119.
[11] Zhang L, Hu Y, Jiang X, Yang C, Lu W, Yang YH. Camptothecin derivative-loaded poly;caprolactone-co-lactide:-b-PEG-b-poly;caprolactone-co-lactide: nanoparticles and their biodistribution in mice. J. Control. Release. 2004;96:135–148.
[12] Chan L, Lee H, Heng P. Production of alginate microspheres by internal gelation using an emulsifica-tion method. Int. J. Pharm. 2002;242:259–562.
[13] Rastogi R, Sultana Y, Aqil M, A Ali, Kumar S, Chuttani K, Mishra A.K. Alginate microspheres of isoniazid for oral sustained drug delivery. Int. J. Pharm. 2007;334:71–77.
[14] Gombotz WR, Wee S. Protein release from al-ginate matrices. Adv. Drug. Deliv. Rev. 1998;31:267–285.
[15] Coppi G, Iannuccelli V, Leo E, Bernabei M.T, Cameroni R. Protein immobilization in crosslinked alginate microparticles. J. Microencapsul. 2002;19:37–44.
[16] Gonzalez-Rodriguez ML, Holgado MA, Sanchez-Lafuente C, Rabasco AM, Fini A. Algi-nate/chitosan particulate systems for sodium diclofe-nac release. Int. J. Pharm. 2002;232:225–234.
[17] Racovita S, Vasiliu S, Popa M, Luca C. Polysaccharides based on micro-and nanoparticles obtained by ionic gelation and their applications as drug delivery systems. Revue. Roumaine .de Chimie. 2009;54:709–711.
[18] Derakhshandeh K, Erfan M, Dadashzadeh S. Encapsulation of 9-nitrocamptothecin, a novel anti-cancer drug, in biodegradable nanoparticles: factorial design, characterization and release kinetics. Eur. J. Pharm. Biopharm. 2007;66:34–41.
[19] Lewis GA. Optimization methods. In: Swarbrick J, Boylan JC, editors. Encyclopedia of pharmaceutical technology. 2nd ed. New York: Marcel Dekker; 2002;21:922–1937.
[20] Seth AK, Misra A. Mathematical modelling of preparation of acyclovir liposomes: reverse phase eva-poration method. J. Pharm. Pharm .Sci. 2002;5:285–291.
[21] Hosseini SM, Amiri M, Najarian S, Dargahi J. Application of artificial neural networks for the esti-mation of tumour characteristics in biological tissues. Int .J. Med. Robot. 2007;3:235–244.
[22] Rafienia M, Amiri M, Janmaleki M, Sadeg-hian A. Application of Artificial Neural Networks in controlled drug delivery Systems. Applied. Artificial. Intelligence. 2010;24:807–820.
[23] Specht DF. A general regression neural network. IEEE. Trans. Neural. Netw. 1991;2:568–576.
[24] Wachowiak MP, Elmaghraby AS, Smoli-kova R, Zurada JM. Generalized regression neural net-works for biomedical image interpolation. Int. Joint. Conf. on. Neural. Networks. ;IJCNN. 2001: 2133-2138.
[25] Amiri M, Saeb S, Yazdanpanah MJ, Seyyedsalehi SA. Analysis of the dynamical behavior of feedback auto-associative memory. Neurocomputing. 2008;71:486–494.
[26] Amiri M, Davandeh H, Sadeghian A, Char-tier S. Feedback associative memory based on a new hybrid model of generalized regression and self-feedback neural networks. Neural. Network. 2010;23:892–904.

[27] Chen T, Chen H. Universal approximation to nonlinear operators by neural networks witharbitrary. Activation functions and its application to dynamical system. IEEE Trans. Neural Networks. 1995;6:911–917.
[28] Khandai M, Chakraborty S, Sharma A, Pan-da D, Khanam N, Kumar PS. Development of propra-nol hydrochlorid matrix tablet: an investigation on ef-fects of combination of hydrophilic and hydrophobic matrix formersusing multiple comparison analysis. 1 ;2010: 2-4.
[29] Ravi PR, Kotreka UK, Saha RN. Controlled release matrix tablets of zidovudine: effect of formulation variables on the in vitro drug release kinetics. AAPS Pharm. Sci. Tech. 2008;9:302–13.
[30] Davande H, Amiri M, Sadeghian A, Chartier S. Feedback associative memory based on a new hybrid model of generalized regression and self-feedback neural networks. Neural. Netw. 2010;23:892–904.
[31] Amrouche A, Rouvaen JM. Efficient system for speech recognition using general regression neural network. International Journal of Computer Systems Science and Engineering. 2006;2:183–189.
[32] Simon L, Frenandes M. Neural network-based prediction and optimization of estradiol release from ethylene-vinyl acetate membranes. Comp. Chem. Eng. 2004;28:2407–2419.
[33] Attama AA, Nwabunze OJ. Mucuna gum microspheres for oral delivery of glibenclamide: In vitro evaluation. Acta. Pharm. 2007;57:161–171.
[34] Bozdag S, Calis S, Kas HS, Ercan MT, Peksoy I, Hincal AA. In vitro evaluation and intra-articular administration of biodegradable microspheres containing naproxen sodium. J. Microencapsul. 2001;18:443–456.
[35] Albarghouthi M, Fara DA, Saleem M, El-Thaher T, Matalka K, Badwan A. Immobilization of antibodies on alginate-chitosan beads. Int. J. Pharm. 2000;206:23–34.
[36] Degroot AR, Neufeld RJ. Encapsulation of urease in alginate beads and protection from α- chy-motripsin with chitosan membranes. Enzyme. Microb. Technol. 2001;29:321–327.

